Novel Low-Density Structure for Hard Rods with Adhesive End Groups

Raghunath Chelakkot, Reinhard Lipowsky, and Thomas Gruhn*

Max Planck Institute for Colloids and Interfaces, Science Park Golm, D-14424 Potsdam, Germany

Received March 26, 2006; Revised Manuscript Received July 13, 2006

ABSTRACT: A system of hard rods with mutually attractive or sticky ends is investigated with the help of Monte Carlo simulations. For low strengths of the attractive interaction, the system behaves qualitatively similar to a hard rod system. At low densities and sufficiently high adhesive strengths, a novel scaffold-like phase is found, which is characterized by a large number of triangles formed by three mutually adhering rods. For a moderate adhesive strength, the scaffold structure is rather flexible, as revealed by lifetime measurements of adhesive contacts. At higher pressure and high adhesive strength, the system forms small smectic-like bundles. At pressures for which the hard rod system becomes nematic, the rods with attractive ends form a smectic A phase, if the adhesive strength is large enough.

1. Introduction

Rodlike colloidal structures, such as rod-shaped viruses, bacilli, or microfilaments[1] are abundant in nature. With modern methods of synthesis one can produce colloidal rods like Boehmite and silicon needles,[2,3] cylindrical dendrimers,[4] and polymeric rods[5] in large amounts. Already in the 1940s, Onsager showed that an isotropic dispersion of hard, infinitely long rods, must undergo a first order orientational ordering transition at sufficiently high density.[6] Later, systems of hard spherocylinders (HSC) were studied extensively with the help of Monte Carlo (MC) simulations. Over the years, the complete phase diagram, which includes isotropic, nematic, smectic, and several crystalline phases, has been determined.[7,8]

In the experimental and theoretical studies of systems of rodlike molecules, a lot of attention has been paid to the high-density region where the system shows global orientational order. However, interesting ordering effects are also visible at low densities in diffusion-limited cluster aggregation[9] and at the percolation threshold[10] of aspherical molecules. The shape anisotropy of the molecules, which leads to the mesophases at higher densities, also induces a large class of structures at low rod concentrations. The structure formation at low densities depends sensitively on the attractive rod−rod interaction. By modifying the HSC model, attractive interactions between the rods can be considered, which allow to study model systems of self-assembling chemical and biological systems.

In this article, Monte Carlo simulations are used to investigate a system of hard rods with adhesive regions at both ends. Such chemically heterogeneous rods are likely to form structures at rather low densities. For example, polar amphiphilic molecules form micelles, membranes or vesicles. As shown in this article, rods with two attractive ends form a scaffold-like phase at low densities. The structure of the scaffold is rather flexible, similar to the filament network of the cytoskeleton of cells (see, for example, ref 11). One realization for our model rods is provided by very stiff telechelic block copolymers, which consist of a long soluble central block and two short hydrophobic end blocks.[12,13] The end groups of telechelic block copolymers form clusters that, interconnected by central blocks, build a three-dimensional, basically amorphous gel phase. The novel aspect in our model is the stiffness of the hydrophilic part which leads to the scaffold-like gel phase, that shows a high local order at low concentrations. At higher rod densities, the scaffold structure collapses and the rods form a smectic structure. Simulations have been performed for various values of the pressure and the strength of the attractive square-well potential, which can be summarized in a global phase diagram.

2. Model and Simulation Method

We consider a monodisperse system of N hard spherocylinders with adhesive ends. Each spherocylinder consists of a cylinder of length l and diameter d and two-half spheres of radius $d/2$ attached to the ends. The configuration of a single spherocylinder labeled by index j is determined by its center of mass $\mathbf{r}_j$ and a unit vector $\mathbf{u}_j$ parallel to the cylinder axis, which points from $\mathbf{r}_j - (l/2)\mathbf{u}_j$ to $\mathbf{r}_j + (l/2)\ \mathbf{u}_j$. The shortest distance

$$\lambda_{ij} \equiv \min_{\substack{-1\le s_i\le 1\\ -1\le s_j\le 1}} ||\left(\mathbf{r}_j + \frac{s_j\, l}{2}\mathbf{u}_j\right) - \left(\mathbf{r}_i + \frac{s_i\, l}{2}\mathbf{u}_i\right)|| \tag{1}$$

between the cylinder axes of rods i and j defines the hard core potential

$$U_{hc} \equiv \begin{cases} 0 & \text{if } \lambda_{ij} \ge d \\ \infty & \text{if } \lambda_{ij} < d \end{cases} \tag{2}$$

between two rods.

Furthermore, an attractive square-well potential

$$U_{sw}\,(||\mathbf{q}_j - \mathbf{q}_i||) \equiv \begin{cases} -\epsilon & \text{if } ||\mathbf{q}_j - \mathbf{q}_i|| < a \\ 0 & \text{if } ||\mathbf{q}_j - \mathbf{q}_i|| \ge a \end{cases} \tag{3}$$

is considered between all pairs of end points $\mathbf{q}_j^{\pm} \equiv \mathbf{r}_j \pm (l/2)\mathbf{u}_j$ and $\mathbf{q}_i^{\pm} \equiv \mathbf{r}_i \pm (l/2)\mathbf{u}_i$ of the cylinder axes of rods i and j. Therefore, the total interaction between two rods i and j is given by

$$U_{ij} \equiv U_{hc}(\lambda_{ij}) + \sum_{\alpha_i=\pm 1}\sum_{\alpha_j=\pm 1} U_{\mathrm{sw}}\left(\left|\left|\left(\mathbf{r}_i + \frac{\alpha_i l}{2}\mathbf{u}_i\right) - \left(\mathbf{r}_j + \frac{\alpha_j l}{2}\mathbf{u}_j\right)\right|\right|\right) \tag{4}$$

In the simulations, the range a of the square well potential is set to $a = 1.2d$, while various values for the adhesive strength ϵ are considered.

Previous studies on systems of hard rods without adhesive interactions have shown that hard rods with higher shape anisotropy exhibit a much richer phase diagram than systems of rods with an

10.1021/ma060680b CCC: $33.50
Published on Web 09/07/2006

almost spherical geometry.[7,8] MC studies revealed that smectic phases appear in a system for rods with aspect ratio $l/d \gtrsim 3.2$ while nematic phases occur for $l/d \gtrsim 3.5$. For rods with an aspect ratio $l/d = 5$, nematic and smectic phases are present in a relatively wide density range.[8] In this article, the influence of attractive ends are investigated for rods with the latter aspect ratio $l/d = 5$. For this purpose, isothermal−isobaric (NPT) Monte Carlo simulations are performed, in which the pressure is chosen as a control parameter, and the system is allowed to level off at an equilibrium density by successive trial changes of the volume. Considering a system of colloidal rods dissolved in water, which is not taken into account explicitly here, the pressure must be taken as a partial pressure, which acts exclusively on the rods. One Monte Carlo sweep includes N trial rod moves, both orientational and translational, plus one trial volume move. In the following we use the reduced pressure $P^* \equiv P v_{sc}/T$ where $v_{sc} \equiv \pi d^3/6 + \pi l d^2/4$ is the hard core volume of a spherocylinder and T is expressed in energy units, in which the Boltzmann constant is absorbed.

To prepare initial configurations, we start with perfectly aligned HSC rods whose centers of mass are located on an fcc lattice, which is scaled along the rod axis by a factor $(1 + l/d)$. The rod axes are oriented perpendicular to the 111 plane of the unscaled lattice. In the absence of attractive interactions, this configuration is equilibrated for various pressures until the equilibrium HSC phase is reached. For each pressure, a series of simulations with the additional square well potential is performed with a stepwise increase of the adhesive strength ϵ. For each ϵ the system is equilibrated before averages are sampled. Tracing in the opposite direction with $\Delta\epsilon < 0$ is used to check hysteresis effects. The number of sweeps needed to equilibrate the system depends on the value of ϵ. For values of $\epsilon < 3.0T$, the system typically equilibrates in 6×10^5 sweeps. For $\epsilon = 4.0T$, the system is equilibrated after 2×10^6 sweeps. For even higher values of ϵ, the number of accepted rod rearrangements decreases and ergodicity is no longer guaranteed.

3. Results

We investigate systems of hard rods with $l/d = 5$, which interact through an attractive square well potential of depth ϵ at the ends of the cylinder axes. Simulations are performed for different values of ϵ and the reduced pressure P^*. For low values of ϵ, the system behaves basically like the HSC system. However, above a certain value $\tilde{\epsilon}$, that depends on P^*, the system behaves qualitatively different. Especially, for low pressures the system forms an interesting new structure.

3.1. Scaffold Phase. We begin with systems at low pressures $P^* < 4.9$ resulting in a volume fraction $\eta < 0.4$ with $\eta \equiv \rho v_{sc}$, where ρ is the density and v_{sc} is the volume of the spherocylinder as before. For low values of the adhesive strength ϵ, the system is in an isotropic fluid state, as known from the HSC system. When ϵ is increased above a threshold value $\tilde{\epsilon}(P^*)$, the rods start to aggregate and a complex scaffold-like structure forms in the system. In the following, we call it the scaffold phase. Figure 1 shows a typical configuration of this phase which is characterized by three structural properties. The most unique structural property of the scaffold phase is the formation of triangles consisting of three rods which are mutually adhering at their headgroups. In a real system an adhesive contact of two headgroups could be mediated by hydrogen bonds, van der Waals forces, entropic effects, specific lock-key interactions or a combination of several mechanisms. In the following, the adhesive contact of two headgroups is called a "bond" . Two adjacent rods can form "bonds" on both ends. Corresponding smectic-like bundles of two or more parallel rods are a second feature of the scaffold phase. A third structural property is the occurrence of end group clusters, at which the ends of several not necessarily parallel rods meet. To investigate the structural properties of the scaffold phase, we introduce the following three order parameters.

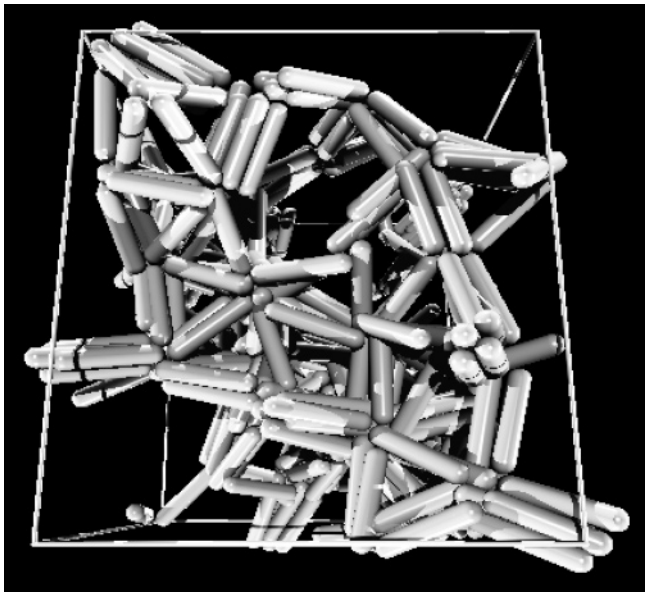

Figure 1. Typical configuration of the scaffold phase for reduced pressure $P^* = 1.34$ and an adhesive strength $\epsilon = 2.5T$.

1. The first is the average number, $\langle N_c \rangle$, of rods sharing one end group cluster. The smallest end group cluster consists of two end groups which form a "bond". In general, an end group cluster consists of all end groups that form a bond with another member of the end group cluster.

2. Then there is the average fraction, $\langle n_d \rangle$, of rods that are involved in small smectic-like bundles, in which adjacent rods adhere to each other on both ends.

3. Finally there is the average number, $\langle N_T \rangle$, of triangle structures formed by three or more rods.

Note that the triangle configuration can involve more than three rods if the edges are formed by bundles. As shown in Figure 2, all three order parameters are close to zero for low values of ϵ. Above a certain value $\epsilon = \tilde{\epsilon}(P^*)$ all three order parameters increase abruptly and denote the spontaneous appearance of the respective structures in the system. If ϵ is increased further, the three order parameters increase only slowly.

If the system undergoes a genuine phase transition, the abrupt increase of the order parameters suggests a first-order transition, but moving the system in the reverse direction from large to small values of ϵ revealed very small hysteresis effects. For a precise characterization of this transition more detailed studies will be necessary.

3.2. Lifetime Distribution of Adhesive Contacts. The scaffold phase is similar to a gel. In the scaffold phase, the "bonds" between the rod ends provide a distinct short-scale order, while on a longer scale the structure is rather amorphous. Apparently, there exists a large number of locally ordered scaffold structures, which are separated by more or less high free energy barriers. It is important to investigate how easily the system can rearrange in the Monte Carlo simulation. Therefore, we computed the lifetime of each "bond" in terms of Monte Carlo sweeps. The results also indicate the flexibility of the real system, even though the "dynamics" of the Monte Carlo simulation differs from the real dynamics, especially because the ratio between translation and rotation attempts of rods could not be adapted to the translational and rotational

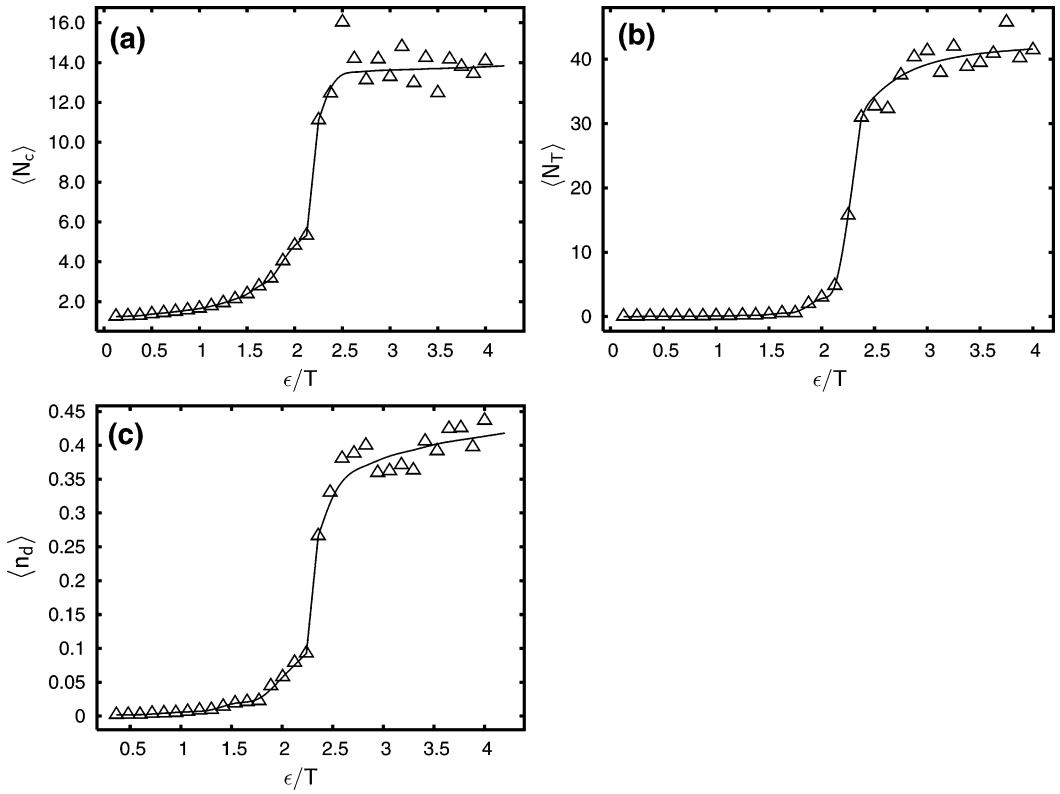

Figure 2. Order parameters of the scaffold phase as a function of the adhesive strength ϵ for a reduced pressure $P^* = 1.34$. (a) The average number of rods, $\langle N_c \rangle$, sharing one end group cluster. (b) The average number of triangles $\langle N_T \rangle$. (c) The average fraction of rods, $\langle n_d \rangle$, participating in a smectic-like bundle.

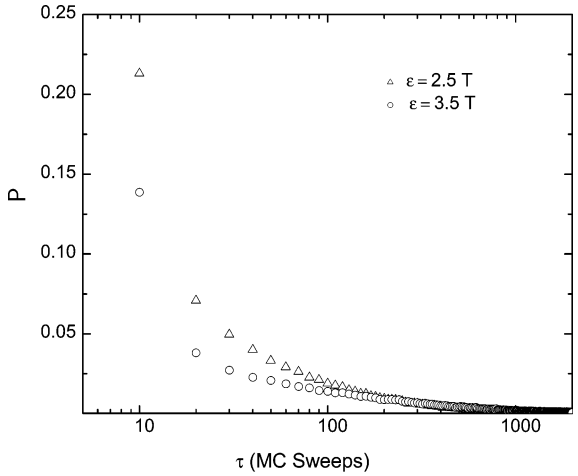

Figure 3. Distribution p of lifetimes τ of "bonds" in a system with adhesive strength $\epsilon = 2.5T$ and $\epsilon = 3.5T$.

diffusion times in the real system which remain to be determined experimentally.

Results are discussed for the reduced pressure $P^* = 1.34$. The probability $p(\tau)$ that a "bond" between two rods lasts for exactly τ sweeps is shown in Figure 3 for $\epsilon = 2.5T$ and $\epsilon = 3.5T$. The graphs of $p(\tau)$ cannot be fitted by a single-exponential function, which indicates that there are more than one characteristic time scales for the duration of "bonds" . The distribution decays fast for short lifetimes, but for $\tau \gtrsim 80$ the decay is strongly diminished.

For $\epsilon = 2.5T$, the structure in the system is very flexible, and lifetimes of "bonds" are very short. More than 20% percent of the "bonds" last no longer than 10 MC sweeps. More than 50% of the "bonds" have lifetimes shorter than 100 MC sweeps. Less than 5% of the "bonds" have lifetimes longer than 2000 MC sweeps.

The average lifetime of the "bonds" increases with increasing ϵ. Lifetime statistics for $\epsilon = 3.5T$ show that the number of "bond" breaks registered in 10^5 sweeps decreased by about 45% compared to a system with $\epsilon = 2.5T$. For $\epsilon > 4.0T$, more than 50% of the "bonds" have lifetimes that exceed 20000 MC sweeps.

3.3. Stability of a Perfect Crystalline Scaffold. The scaffold phase is characterized by a globally irregular, scaffold-like structure with triangular arrangements of the rods. Furthermore, tetrahedral clusters are formed, in which rods build the edges, connecting the four vertexes. The regular tetrahedron can be used to create a space-filling crystalline structure with an fcc symmetry. The centers of mass of a conventional fcc crystal are the locations of end group clusters in the scaffold crystal which are connected by the rods. It is interesting to test whether the crystalline scaffold structure is a stable state of the system or whether the less ordered gellike scaffold phase is preferred. Therefore, simulations were performed which started from an ideal scaffold crystal configuration. In the initial configuration the rods connect points, arranged in an fcc lattice with a lattice constant $l/d + 1$. The rods are arranged in such a way that each fcc lattice point is connected with it's nearest neighbors, as shown in Figure 4a.

For each "bond" between rods with indices i and j we measure the angle $\theta_{ij} \equiv \arccos(\mathbf{u}_i \cdot \mathbf{u}_j)$ between the unit vectors $\mathbf{u}_i$ and $\mathbf{u}_j$ which are parallel to the rod axes and point away from the "bond". In the crystalline scaffold structure, the angle θ_{ij} between two rods with mutually adhering end groups is $\pi/3$. In our simulation the scaffold crystal consists of 576 rods. The volume fraction of the initial state is $\eta \simeq 0.14$. Simulations are performed with different values of ϵ. For $\epsilon < \tilde{\epsilon}$, the crystalline initial configuration is unstable and melts into an isotropic fluid

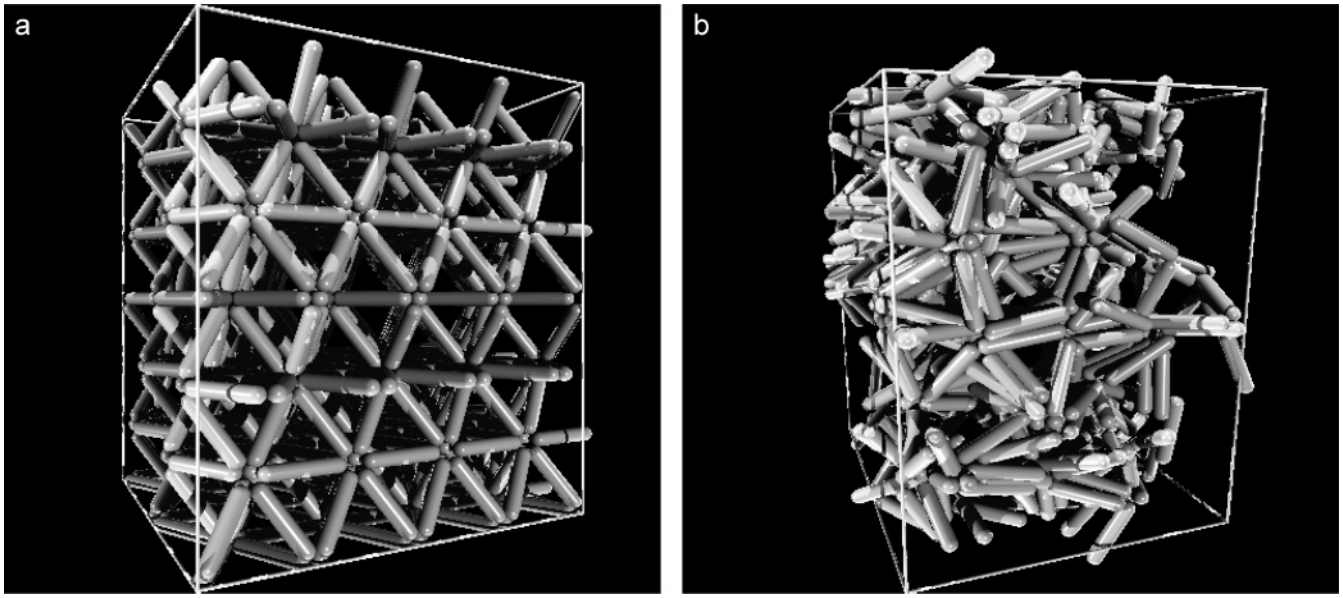

Figure 4. (a) Initial crystalline scaffold configuration. (b) Confuguration for an adhesive strength $\epsilon = 2.5T$, where the crystalline scaffold becomes unstable and collapses to the scaffold phase structure.

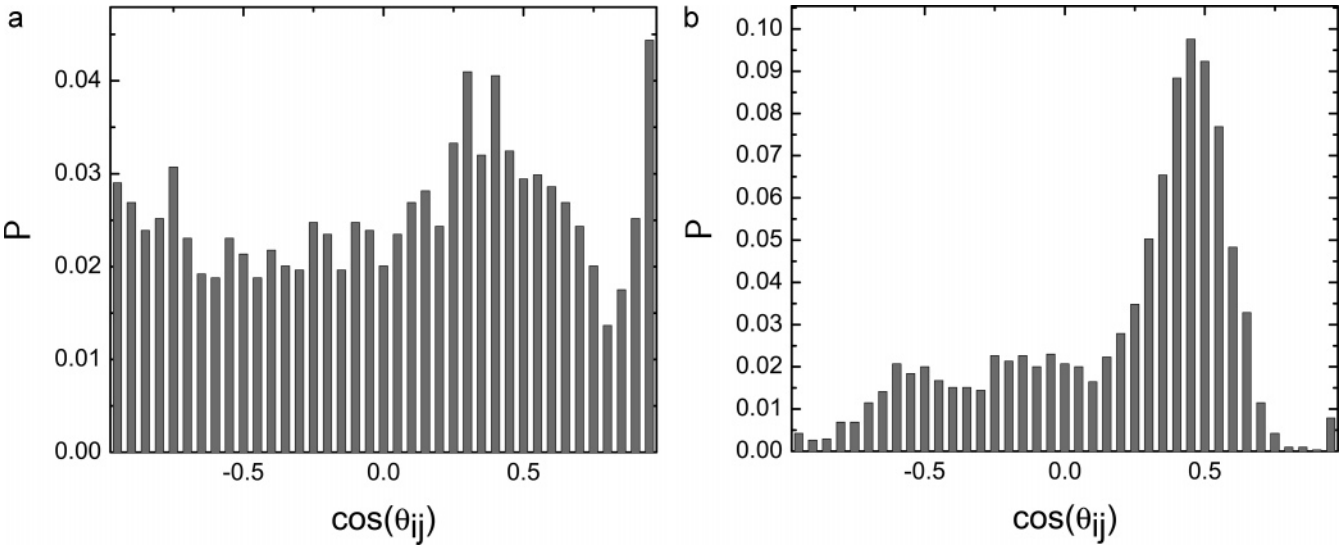

Figure 5. Distribution p of angles θ_{ij} between mutually adhering rods for a relaxated system obtained from an initial crystalline scaffold configuration with adhesive strength (a) $\epsilon = 2.5T$ and (b) $\epsilon = 5.0T$.

phase. For $\epsilon > \tilde{\epsilon}$, the crystalline configuration melts again, but now into the scaffold phase, indicating that the scaffold phase is, indeed, the favorite structure for $\epsilon > \tilde{\epsilon}$ (see Figure 4b). In Figure 5, histograms for the angle θ_{ij} are shown for systems started from the ideal crystalline scaffold. For $\epsilon = 2.5T$, as in Figure 5a, the distribution of $\cos(\theta_{ij})$ for the equilibrated system shows the typical order of the gellike scaffold phase. The peak at $\cos(\theta_{ij}) = 1$ stems from the nearly parallel rods in the bundles. A broad maximum around $\cos(\theta_{ij} = \pi/3) = {}^1/_2$ is caused by the triangle configurations in the gellike scaffold phase. Only if ϵ is increased up to $5T$, as in Figure 5b, the angle distribution shows a distinct maximum around $\cos(\theta_{ij}) = {}^1/_2$, indicating the structure of the crystalline scaffold. However, in this ϵ region the acceptance rates are low and so the system might be caught in a metastable state.

It is noteworthy that in the range of $\tilde{\epsilon} < \epsilon < 5T$ and $P^* \lesssim 4.5$ the same scaffold phase is obtained from two rather different starting configurations; the isotropic phase and the ideal scaffold crystal. This corroborates the point that within this parameter region the scaffold phase is stable.

3.4. Simulations at Higher Pressure. For the reduced pressure $P^* = 4.9$, the HSC system is in a dense isotropic phase with a volume fraction $\eta \simeq 0.4$. For low values of ϵ, the system of rods with adhesive ends behaves in a qualitatively similar manner. Above a threshold value $\tilde{\epsilon}(P^* = 4.9) \simeq 1.5T$, the rods aggregate to form small smectic-like bundles. On a larger scale, however, the system shows no global orientational order (Figure 6a). The density is distinctly higher than in the scaffold phase, which prevents the formation of the space consuming triangular configurations. As a consequence, the average number of triangles decreases drastically as shown in Figure 7. At higher pressures $5.4 \lesssim P^* \lesssim 6.7$, the HSC system becomes nematic. If ϵ is increased above the threshold value $\tilde{\epsilon}(P^*)$, the system performs a phase transition from the nematic to a smectic A phase (Figure 6b). Figure 8 shows $g_{||}(r_{||})$, the pair correlation function along the direction of the rod axis. For a reference rod

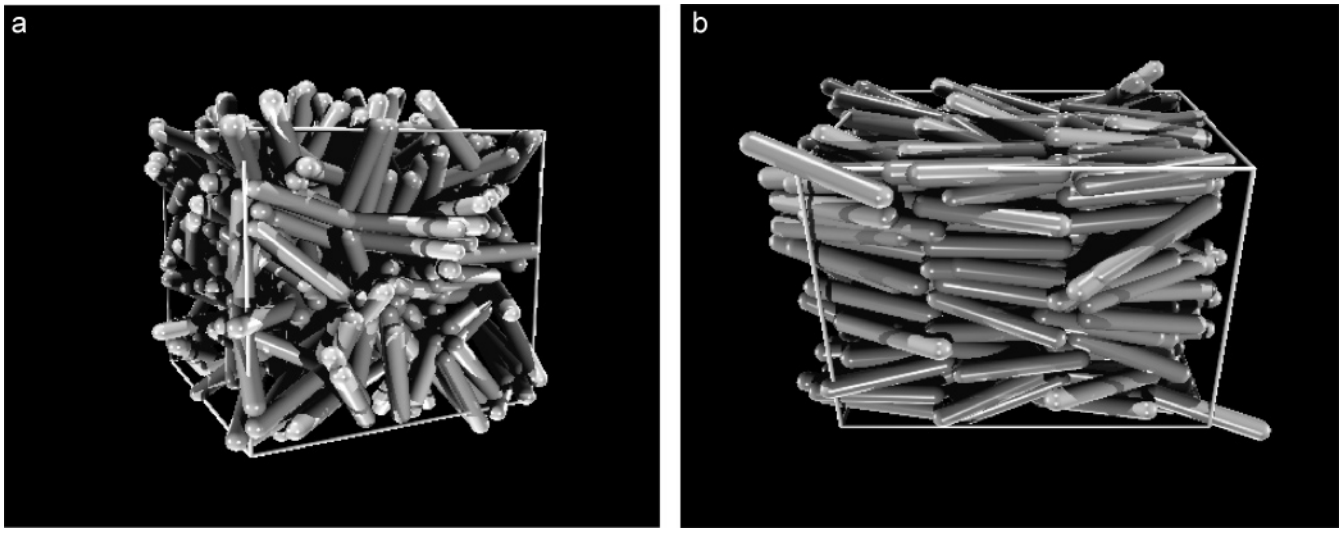

Figure 6. (a) Globally isotropic phase with small smectic bundles. (b) Smectic phase obtained for a reduced pressure $P^* = 5.78$, and an adhesive strength $\epsilon = 2.25T$.

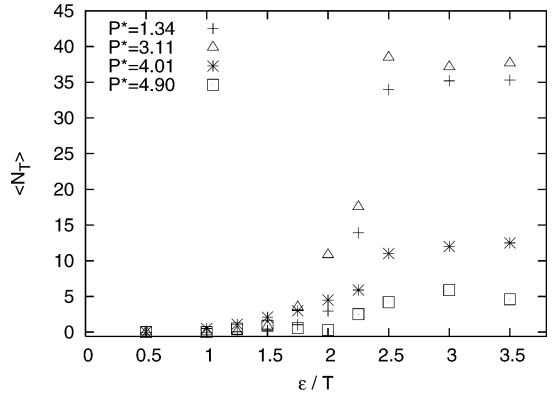

Figure 7. Average number of triangles as a function of the adhesive strength ϵ for different values of the reduced pressure P^*.

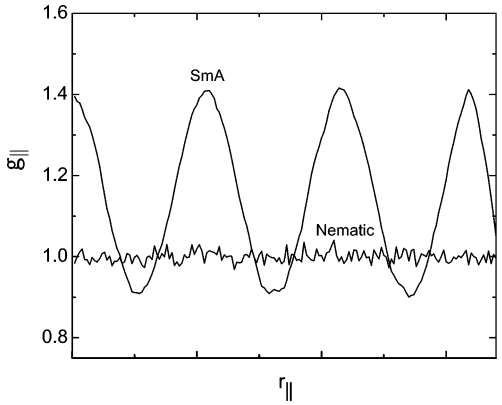

Figure 8. Pair correlation function $g_{||}$ projected along the rod axis as a function of the distance $r_{||}$ from the reference rod.

with a center of mass at $\boldsymbol{r}$ and a rod axis parallel to the unit vector $\mathbf{u}$ the function $g_{||}(r_{||})$ denotes the local density in a small volume around $\mathbf{r} \pm r_{||}\mathbf{u}$ divided by the overall density. The periodic oscillations of $g_{||}(r_{||})$ identify the smectic layering.

With all the data collected from the simulation, a phase diagram has been constructed.

4. Phase Diagram

Systems of hard rods with adhesive end groups have been investigated here for a wide range of reduced pressure P^* and adhesive strength ϵ. In Figure 9, our results are summarized in a phase diagram. Symbols denote the points where the respective phases were determined. Lines are added to indicate the phase boundaries. A more detailed localization of the phase boundaries as well as determination of the order of the transitions requires a more refined study with umbrella sampling or equivalent methods[14] which have not been applied yet. The phase diagram shows a phase boundary separating the diagram into a low ϵ and a high ϵ region. For values of $\epsilon < \tilde{\epsilon}(P^*)$, the system behaves qualitatively similar to the HSC system, which means it is isotropic for $P^* \lesssim 5.7$ and nematic for $5.75 \lesssim P^* \lesssim 6.7$. For $\epsilon > \tilde{\epsilon}(P^*)$, three different states are found, depending on the pressure P^*. For $P^* \lesssim 4.5$ and corresponding volume fractions $\eta \lesssim 0.37$ the system is in the scaffold phase, showing a scaffold like three-dimensional structure with characteristic triangular rod configurations. Around $P^* \simeq 5$ and a corresponding volume fraction $\eta \simeq 0.4$, the rods form small smectic-like bundles but the system shows no global orientational order. In this high density structure the number of triangles is distinctly lower than

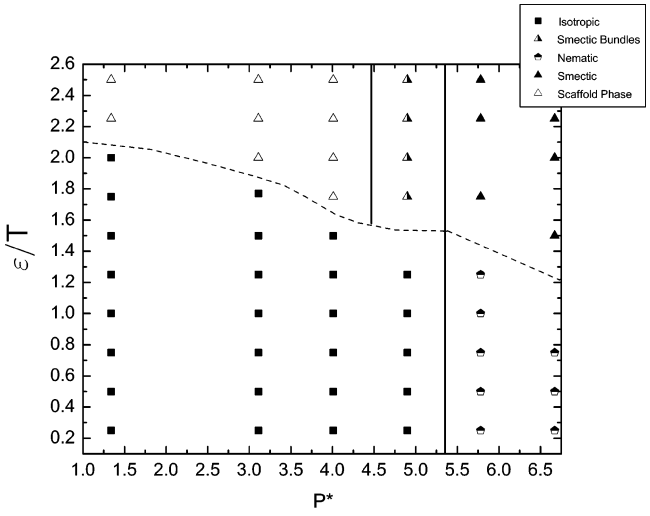

Figure 9. Phase diagram for hard rods with adhesive ends as a function of the reduced pressure P^* and the adhesive strength ϵ in units of T. The dashed line represents the phase boundary $\tilde{\epsilon}(P^*)$. Below the dashed line, the system is in the isotropic phase for low pressures and in the nematic phase for higher pressure values. Above the dashed line, the system is in the scaffold phase for low pressures, and in the smectic A phase for sufficiently high pressures. Between the scaffold phase and the smectic A phase, the system forms small smectic-like bundles, while triangular structures are strongly neglected.

in the scaffold phase. For pressures $P^* \gtrsim 5.5$, a smectic A phase is formed for $\epsilon > \tilde{\epsilon}$.

5. Conclusions

A novel scaffold-like phase has been found for a monodisperse system of hard spherocylindrical colloids with short range attractive potentials at both ends. The new gellike phase, which is characterized by the occurrence of triangular clusters, shows a high degree of order at extremely low densities. Even though this is the first investigation of the scaffold phase and many details remain to be explored, the unusual properties of this new material already point toward various possible applications.

The superporous scaffold structure combines an exceptionally large surface with local order. As known from zeolites and metal−organic coordination networks, these are excellent properties for high-efficiency catalysis or molecular recognition.[15,16] Using electrically conducting rods, the scaffold structure might also serve as a flexible, strongly interconnected nanowire network (compare with ref 17). Since the scaffold phase is bicontinuous, it provides a three-dimensional transport system in the cavities and may serve at the same time as a three-dimensional transport system for molecular motors which can walk along the rods.[18]

The ideal crystalline scaffold configuration has been found to be unstable for adhesive strengths up to $\epsilon \lesssim 5T$. For $\epsilon = 5T$, the crystalline structure is more persistent. However, the thermodynamic stability of the crystalline structure for $\epsilon \geq 5T$ could not be shown here, since the acceptance rates for Monte Carlo steps become very low for high values of ϵ. It would be an interesting task to address this open issue using simulation techniques that are specialized to the analysis of solid crystals.

Note Added in Proof. The term "scaffold phase" is used here in the same sense as "scaffold structure". At present, we cannot decide if the abrupt changes displayed in Figure 2 indicate a genuine phase transition.

Acknowledgment. Support by the Deutsche Forschungsgemeinschaft via the Sonderforschungsbereich 448 is gratefully acknowledged.

References and Notes

(1) Gould, J. L.; Keeton, W. T. *Biological Science*, 6th ed.; W. W. Norton & Company: New York and London, 1996.
(2) Buining, P. A.; Pathmamanoharan, C.; Jansen, J. B. H.; Lekkerkerker, H. N. W. *J. Am. Ceram. Soc.* **1991**, *74*, 1303.
(3) van Katz, C. M.; Johnson, P. M.; van den Meerakker, J. E. A. M.; van Blaaderen, A. *Langmuir* **2004**, *20*, 11201.
(4) Schlüter, A. D.; Rabe, J. P. *Angew. Chem., Int. Ed.* **2000**, *39*, 864.
(5) Alargova, R. G.; Bhatt, K. H.; Paunov, V. N.; Velev, O. D. *Adv. Mater.* **2004**, *18*, 1653.
(6) Onsager, L. *Ann. N.Y. Acad. Sci.* **1949**, *51*, 627.
(7) Bolhuis, P.; Frenkel, D. *J. Chem. Phys.* **1997**, *106*, 666.
(8) McGrother, S. C.; Williamson, D. V.; Jackson, G. *J. Chem. Phys.* **1996**, *104*, 6755.
(9) Mohraz, A.; Moler, D. B.; Ziff, R. M.; Solomon, M. J. *Phys. Rev. Lett.* **2004**, *92*, 155503.
(10) Garboczi, E. J.; Snyder, K. A.; Douglas, J. F.; Thorpe, M. F. *Phys. Rev. E* **1995**, *52*, 819.
(11) Satcher, R. L., Jr.; Dewey, C. F., Jr. *Biophys. J.* **1996**, *71*, 109.
(12) Preuschen, J.; Menchen, S.; Winnik, N. A.; Heuer, A.; Spiess, H. W. *Macromolecules* **1999**, *32*, 2690.
(13) Khalatur, P. G.; Khokhlov, A. R.; Kovalenko, J. N.; Mologin, D. A. *J. Chem. Phys.* **1999**, *110*, 6039.
(14) Frenkel, D.; Smit, B. *Understanding Molecular Simulation*, 2nd ed.; Academic Press: San Diego, CA, 2002.
(15) Seo, J. S.; Whang, D.; Lee, H.; Jun, S. I.; Oh, J.; Jeon, Y. J.; Kim, K. *Nature (London)* **2000**, *404*, 982. Evans, O. R.; Ngo, H. L.; Lin, W. *J. Am. Chem. Soc.* **2001**, *123*, 10395.
(16) Zhao, G.; Teng, J.; Zhang, Y.; Xie, Z.; Yue, Y.; Chen, Q.; Tang, Y. *Appl. Catal., A: Gen.* **2006**, *299*, 167. Dimitrova, R.; Gündüz, G.; Spassova, M. *J. Mol. A: Chem.* **2006**, *243*, 17. Jancen, J.; Creyghton, E.; Njo, S.; van Koningsveld, H.; van Bekkum, H. *Catal. Today* **1997**, *38*, 205.
(17) Cao, X. B.; Xie, Y.; Li, L. Y. *Adv. Mater.* **2003**, *15*, 1914.
(18) Klumpp, S.; Nieuwenhuizen, T. M.; Lipowsky, R. *Biophys. J.* **2005**, *88*, 3118.

MA060680B